Optimal balancing of xylem efficiency and safety explains plant vulnerability to drought

Oskar Franklin[1,2] | Peter Fransson[2,3] | Florian Hofhansl[1] | Steven Jansen[4] | Jaideep Joshi[1,5,6,7]

[1]International Institute for Applied Systems Analysis, Laxenburg, Austria

[2]Department of Forest Ecology and Management, Swedish University of Agricultural Sciences, Umeå, Sweden

[3]Interdisciplinary Center for Scientific Computing, Heidelberg University, Heidelberg, Germany

[4]Institute of Botany, Ulm University, Ulm, Germany

[5]Institute of Geography, University of Bern, Bern, Switzerland

[6]Oeschger Centre for Climate Change Research, University of Bern, Bern, Switzerland

[7]Complexity Science and Evolution Unit, Okinawa Institute of Science and Technology Graduate University, Okinawa, Japan

Correspondence
Oskar Franklin and Jaideep Joshi, International Institute for Applied Systems Analysis, Schlossplatz 1, Laxenburg A-2361, Austria.
Email: franklin@iiasa.ac.at and joshi@iiasa.ac.at

Abstract

In vast areas of the world, forests and vegetation are water limited and plant survival depends on the ability to avoid catastrophic hydraulic failure. Therefore, it is remarkable that plants take hydraulic risks by operating at water potentials (ψ) that induce partial failure of the water conduits (xylem). Here we present an eco-evolutionary optimality principle for xylem conduit design that explains this phenomenon based on the hypothesis that conductive efficiency and safety are optimally co-adapted to the environment. The model explains the relationship between the tolerance to negative water potential (ψ_{50}) and the environmentally dependent minimum ψ (ψ_{min}) across a large number of species, and along the xylem pathway within individuals of two species studied. The wider hydraulic safety margin in gymnosperms compared to angiosperms can be explained as an adaptation to a higher susceptibility to accumulation of embolism. The model provides a novel optimality-based perspective on the relationship between xylem safety and efficiency.

KEYWORDS
conductivity, embolism, functional traits, optimality, tracheids, trees, vessels, vulnerability, xylem

INTRODUCTION

The hydraulic properties of plants constrain their ability to grow and survive in different environments. Therefore, a solid understanding of these constraints is essential for accurate prediction of vegetation responses to droughts and other environmental changes. In stems, the primary function of the xylem is to transport water, driven by the difference in water potential between the base and the top. Plants regulate water transport via stomatal conductance in order to avoid highly negative water potentials (i.e. with xylem sap under negative pressure) that could induce xylem embolism, with associated loss of conductivity. The sensitivity to embolism is often measured in terms

of the water potential at which conductivity is reduced by 50%, ψ_{50}. Across a large number of angiosperm species, ψ_{50} was found to be close to the minimum midday water potential (ψ_{min}) experienced by each species, implying a remarkably narrow hydraulic safety margin ($\psi_{50} - \psi_{min}$) (Choat et al., 2012). The safety margin is smaller for angiosperms than gymnosperms, and is smallest in wet sites with high ψ_{min}. Although recent studies based on improved methods indicate that hydraulic vulnerability has been overestimated in many species (Lens et al., 2022), conductivity loss due to embolism remains a ubiquitous phenomenon under drought conditions. It has been proposed that this potentially risky strategy is related to a physiological trade-off, so that a higher conductivity is linked to a higher vulnerability, but this has yet been difficult to demonstrate (Gleason et al., 2016; Liu et al., 2021; Sanchez-Martinez et al., 2020). Hence, the regulation of plant hydraulic safety margins is not yet fully understood, despite its importance for our understanding of plant responses to expected climate changes and droughts (Anfodillo & Olson, 2021; Venturas et al., 2017). Here we analyse the variation in ψ_{50} through an eco-evolutionary-optimality perspective.

The basic principle of eco-evolutionary optimality is that traits have adapted towards values that maximize plant fitness in the environment where the plants have evolved (Franklin et al., 2020; Harrison et al., 2021). Due to the unpredictability of environmental variation, no plant will be perfectly optimal, but the principle nevertheless predicts a remarkable portion of observed variation in a wide range of plant traits and processes, including plant stomatal hydraulic regulation (Anderegg et al., 2018; Hölttä et al., 2011; Joshi et al., 2022; Wang et al., 2020; Wolf et al., 2016), vascular network structure (Koçillari et al., 2021; McCulloh et al., 2003; Savage et al., 2010), and leaf hydraulic and photosynthetic traits (Deans et al., 2020). A successful application of eco-evolutionary optimality (EEO) principle requires a sufficient understanding of the fitness benefits and costs of the traits to be modelled. Xylem efficiency and safety in relation to growth environment has only rarely been addressed from an EEO perspective, perhaps due to a lack of consensus on the xylem costs and benefits. For example, Manzoni et al. (2013) used an EEO approach based on the principle that transpiration is maximized, which contrasts to the assumption in most other models that transpiration is a cost (Wang et al., 2017). Another EEO approach was based on the trade-off between increasing xylem conductivity (benefit) and decreasing resistance to embolism (cost) with increasing conduit diameter, which explained stem tip to base widening of conduit diameter in a global data set (Koçillari et al., 2021).

Here we present an EEO model for xylem tissue, based on optimality theory and xylem trait-interrelationships derived from a large xylem functional trait data set (Choat et al., 2012). First, we quantify the effects of key xylem traits—conduit diameter and pit membrane properties—on conductivity and safety, which shows that there is a relationship between xylem efficiency and safety at the level of conduits, even though it does not appear as a strong trade-off at the level of whole sapwood tissue. Then we combine these relationships with an EEO hypothesis that plants maximize the combination of xylem conductive capacity per unit xylem biomass and tolerance to low ψ (ψ_{50}). To account for the full fitness consequences of xylem safety, we also account for the consequences of potential refilling and within-xylem variation in vulnerability among conduits. Our first-principles EEO model explains the globally observed relationship between ψ_{50} and the environmentally dependent ψ_{min}, and suggests explanations for the large difference in hydraulic safety margin between angiosperms and gymnosperms.

MODEL DESCRIPTION AND RESULTS

An optimality perspective for conductive tissue

Our model is based on the eco-evolutionary optimality principle, implying that the xylem traits are adapted to maximize fitness in the plant's environment. Each trait is associated with fitness benefits and costs and the optimal trait values are those that maximize the net benefit. Because the main role of the xylem is to supply water to the leaves, the fitness benefit increases with conductivity. However, xylem conductivity is a complex property that depends not only on its un-stressed maximal conductive capacity (K, [Kg m^{-1} MPa^{-1} s^{-1}]), but also on its ability to withstand stress (low water potential, [MPa]) without losing conductivity (resistance to conductivity loss, P), resulting in a realized conductivity, $K \cdot P$. The main fitness cost of the xylem (and most plant organs) is its construction and maintenance costs, which are proportional to its mass per unit length (M [g m^{-1}]). Combining benefits and cost at the tissue level, the optimal xylem traits should maximize conductivity and safety per biomass, that is $K \cdot P / M$. To evaluate this hypothesis, we need to first determine the key xylem traits that determine the xylem costs and benefits and how they are linked. For this and all other analyses we used a large data set on hydraulic traits (Choat et al., 2012), downloaded from the TRY database (Kattge et al., 2020). The downloaded data set includes many traits additional to those used in the paper by Choat et al. (2012). The data set was further complemented by additional data on pit traits from Kaack et al. (2021) and ψ_{50} versus ψ_{min} from Domec et al. (2009). The combined data set and code used in this study are provided in a supplementary file.

Conduit conductivity and safety

The xylem can be seen as a network of interconnected conduits (vessels or tracheids). Xylem conductivity and

safety (tolerance to negative water potential, ψ_{50} [MPa]) depends on both the conduits themselves and their interconnections, the pits and end-walls (i.e. the overlapping interconduit walls), and how the conduits are spatially clustered (Hacke et al., 2004; Lens et al., 2011; Scholz et al., 2013). Conduit diameter (D, [µm]) is an important determinant of conductivity due to the strong effect on fluid dynamics (Hacke et al., 2017), which is also reflected in the ubiquitous tapering of D with stem height, which serves to minimize the increase in resistance with path length (Anfodillo et al., 2006; Koçillari et al., 2021; West et al., 1999). To account for the disproportionally large contribution of relatively larger conduits across the xylem cross-section, we use hydraulically weighted conduit diameter $D = \frac{\sum_i D_i\,D_i{}^4}{\sum_i D_i{}^4}$ (based on the Hagen–Poiseuille equation for fluid dynamics), rather than the mean diameter ($\overline{D}$). Analogously, we calculate a corresponding hydraulically weighted number of conduits per area $N = \overline{N}\left[\frac{\overline{D}}{D}\right]^4$ based on the reported mean number of conduits per sapwood area ($\overline{N}$, [mm^{-2}]).

We found that conductivity of a conduit (K, maximal conductivity at $\psi = 0$) strongly increases with D ([µm], parameters in Table 1, $r^2 = 0.90$ and 0.78 for angiosperms and gymnosperms, respectively, Table 2). At the same time, some studies have found that pit conductivity between conduits is as important as vessel conductivity for total xylem conductivity (Choat et al., 2008; Wheeler et al., 2005). These findings can be reconciled if pit conductivity is coordinated with D, as shown by the correlation with pit area (total inter-conduit pit-membrane surface area, Table 2). Nevertheless, another pit trait, pit-membrane thickness (T_m [µm]), has been found to have an effect on conductivity independent of D in angiosperms (Lens et al., 2011), probably via the number of pore constrictions in pit membrane pores (Kaack et al., 2019, 2021). The importance of T_m is further underlined by its role for embolism resistance, discussed below (Equation 3). Thus, we assume that in addition to

the strong effect of D, K is potentially influenced by T_m (Table 2, Equation 1).

$$K = c_1\,D^k\,T_m^p. \tag{1}$$

The symbol c_1 in Equation (1) (and likewise $c_2 \ldots c_6$ in the equations further below) denote constants that do not matter for our final results. Because of the scarcity of observations on T_m, we cannot get a reliable empirical estimate of its effect on K (i.e. the exponent p in Equation 1). Instead, we predict a theoretical value based on our optimality criterion, see below.

Xylem safety in response to ψ can be described by a vulnerability function (P), which describes how sapwood conductivity declines relative to its maximal value with negative xylem water potential ψ. Among commonly used xylem vulnerability functions, the Weibull function (Equation 2) has the advantages that it always approaches 1 as $\psi \to 0$ and that its parameter a does not vary significantly with ψ_{50} (Duursma & Choat, 2017).

$$P = \left(\frac{1}{2}\right)^{\left(\frac{\psi}{\psi_{50}}\right)^a}. \tag{2}$$

In Equation (2), ψ_{50} is ψ that causes 50% loss of the maximum conductivity, which is a largely genetically determined functional trait (Lamy et al., 2014; Lobo et al., 2018; Pritzkow et al., 2020), evolutionarily adapted to the environmental conditions experienced by a species (Zhang et al., 2021). The parameter a controls the shape of P, and was estimated based on relationship between ψ_{50} and ψ_{88} (Appendix S1) for each species, from which median values for angiosperms and gymnosperms were estimated (Table 1).

The relative importance of different underlying traits in determining ψ_{50} varies among studies and species, for example pit features and vessel length being most important in *Acer* species (Lens et al., 2011) while D and vessel grouping are important in other species (Levionnois

TABLE 1 Parameters/scaling factors estimated from data. All analyses are based on data from Choat et al. (2012) and available in the TRY database (Kattge et al., 2020) complemented by additional data on pit traits from Kaack et al. (2021).

Symbol	Parameter description	Estimate angiosperms	Estimate gymnosperms
a	Slope parameter of the vulnerability function P (Equation 2)	2.18 ± 0.11, $n = 682$	4.33 ± 0.33, $n = 291$
d	The effect of D on ψ_{50} (Equation 3)	-1.30 ± 0.33, $n = 17$	-0.99 ± 0.17, $n = 41$
t	The effect of T_m on ψ_{50} (Equation 3)	0.58 ± 0.23, $n = 17$	0.33 ± 0.17, $n = 28$
k	The effect of D on K (Equation 1)	3.58 ± 0.18, $n = 47$	3.02 ± 0.32, $n = 27$
m	The effect of D on T_c (Equation 6)	0.49 ± 0.11, $n = 36$	0.21 ± 0.11, $n = 49$
f	The effect of ψ_{50} on T_c (Equation 6)	0.23 ± 0.090, $n = 36$	0.23 ± 0.063, $n = 49$
x	Embolism accumulation parameter (Equation 5)	0.96 ± 0.040, $n = 381$	6.73 ± 1.14, $n = 99$

Note: D: Hydraulically weighted conduit diameter [µm]. T_m: Pit membrane thickness in angiosperms, torus: pit membrane diameter ratio in gymnosperms [µm]. T_c: Conduit wall thickness of conduits with diameter D [µm].

TABLE 2 Inter-trait relationships (linear regressions and standardized major axis regressions (sma)); Ang. = Angiosperms, Gym. = Gymnosperms. All analyses are based on data from Choat et al. (2012) and available in the TRY database (Kattge et al., 2020) complemented by additional data on pit traits from Kaack et al. (2021).

Model	Group	Factor	Estimate	SE	p	R^2	R^2_{adj}	n
sma (pit area ~ $\overline{D}$)	Ang.				<0.001	0.58		81
	Gym.				<0.001	0.60		57
$\ln(K) \sim \ln(D)$	Ang.	$\ln(D)$	3.5832	0.1795	<0.001	0.90	0.90	47
	Gym.	$\ln(D)$	3.0202	0.3208	<0.001	0.78	0.77	27
$\ln(-\Psi_{50}) \sim \ln(D)$	Ang.	$\ln(D)$	−0.7905	0.0926	<0.001	0.29	0.29	178
	Gym.	$\ln(D)$	−0.7339	0.082	<0.001	0.33	0.33	164
$\ln(-\Psi_{50}) \sim \ln(T_m)$	Ang.	$\ln(T_m)$	0.5977	0.0841	<0.001	0.37	0.37	87
	Gym.	$\ln(T_m)$	−0.0114	0.1949	0.954	0	−0.03	37
$\ln(-\Psi_{50}) \sim \ln(D) + \ln(T_m)$	Ang.	$\ln(T_m)$	0.5794	0.236	0.028	0.58	0.53	17
	Ang.	$\ln(D)$	−1.2955	0.3317	0.002	0.58	0.53	17
	Gym.	$\ln(T_m)$	0.3348	0.1678	0.002	0.63	0.61	41
	Gym.	$\ln(D)$	−0.9928	0.1696	<0.001	0.63	0.61	41
sma ($\ln(T_m) \sim \ln(D)$)	Ang.				0.59	0.02	−0.04	20
	Gym.				0.068	0.08	0.06	41
$\ln(T_c) \sim \ln(D_T)$	Ang.	$\ln(D)$	0.4923	0.1154	<0.001	0.35	0.33	36
	Gym.	$\ln(D)$	0.0236	0.1099	0.831	0	−0.02	49
$\ln(T_c) \sim \ln(D_T) + \ln(-\psi_{50})$	Ang.	$\ln(D)$	0.4891	0.1072	<0.001	0.45	0.42	36
	Ang	$\ln(-\psi_{50})$	0.2266	0.0899	0.017	0.45	0.42	36
	Gym	$\ln(D)$	0.2055	0.1086	0.065	0.24	0.2	49
	Gym	$\ln(-\psi_{50})$	0.2348	0.0626	<0.001	0.24	0.2	49

Note: Pit area = Total interconduit pit (membrane) surface area of a conduit [mm²]. $\overline{D}$: Mean conduit diameter [μm]. D: Hydraulically weighted conduit diameter [μm]. D_T: Here D was calculated based on measurements of the ratio T_c/D in order to get D values for the same conduits used to measure T_c. T_m: Pit membrane thickness in angiosperms, torus: pit membrane diameter ratio in gymnosperms [μm]. T_c: Conduit wall thickness of conduits with diameter D [μm].

et al., 2021; Scholz et al., 2013). Recent studies have highlighted the importance of pit membrane thickness in angiosperms (Kaack et al., 2021; Lens et al., 2022) and the ratio between torus diameter and pit aperture or between torus diameter and pit-membrane diameter in gymnosperms (Bouche et al., 2014). Based on our data, we found that in combination with D, the ratio between torus diameter and pit-membrane diameter was the best predictor of ψ_{50} in gymnosperms. For simplicity, we use the same symbol, T_m, to represent both pit-membrane thickness in angiosperms and the ratio between torus and pit-membrane diameter in gymnosperms. Because a mechanism linking D to ψ_{50} has not yet been conclusively identified, it is likely that the effect of D is indirect, e.g. via pit area which is correlated with D (Table 2) and other traits, such as vessel length and interconnectivity between vessels and tracheids (Lens et al., 2022). We found that a combination of D and T_m explains about 60% of the variation in ψ_{50}, which is much more than either D or T_m alone (Equation 3, Table 2). We also found no significant correlation between D and T_m (Table 2), suggesting independent effects on ψ_{50}, as also found by Lens et al. (2022).

$$\psi_{50} = c_2 \, D^d \, T_m^{\,t}. \tag{3}$$

Because K increases and ψ_{50} decreases with D, there should be some degree of trade-off between them,

although the relationship is also influenced by variation in T_m (Equation 4), and likely other unmeasured properties.

$$\psi_{50} = c_3 \, T_m^{\,t-pd/k} \, K^{d/k}. \tag{4}$$

This trade-off (Equation 4), and our model, is defined at the level of conductive tissue (or equivalently, probabilistically at the individual-conduit level) rather than for whole-sapwood tissue. We emphasize that whole-sapwood conductivity also depends on the number of conduits per unit sapwood area ($K_{sapwood} = K_{conduit} \cdot N$), which weakens this relationship at the whole-plant level (Figure 1).

Extended effects of conductivity loss

Measured vulnerability curves (P, Equation 2) represent the instantaneous loss of conductivity due to embolism at the whole xylem level, but the full fitness impact depends also on the accumulation of conductivity loss over the life-time of the functional xylem. Here we consider three parameters that influence embolism accumulation: (1) refilling of embolized conduits. Although the plants' ability to refill conduits is debated and conclusions vary among studies (Anderegg et al., 2013; Avila et al., 2022; Klein et al., 2018; Pellizzari et al., 2016; Rehschuh et al., 2020), we consider its potential role for xylem optimization. (2) The

number of drought (embolism) events expected during the lifetime of the water-conducting xylem. (3) The effect of partial conductivity loss on the average conductivity of the remaining functional xylem. This factor depends on the distribution of vulnerability among individual conduits (Avila et al., 2022). If all conduits are equally vulnerable or the vulnerability of each conduit is stochastic, a random selection of conduits will be embolized in each drought event. Consequently, the vulnerability of the remaining conductive xylem will not change with repeated drought events. This will lead to multiplicative reduction of total conductivity with each embolism event. In contrast, if there is variation in vulnerability among conduits and conduit-level vulnerability is deterministic, the most vulnerable conduits will embolize first. Because the more resistant conduits remain functional, the total xylem vulnerability (ψ_{50}) will decline with the total accumulated loss of conductivity.

Based on these embolism-parameters, the xylem lifetime conductivity-loss function (P_t) can be written as follows:

$$P_t = P^x = P^{in^s} \tag{5}$$

In Equation (5), x is the aggregated embolism accumulation exponent. i is the irreversibility of embolism, potentially varying from no irreversibility ($i=0$, complete refilling and no conductivity loss, i.e. $P_t=1$) to complete irreversibility ($i=1$, no refilling). n is the number of drought events expected during the lifetime of the xylem. s is the stochasticity of embolism in individual conduits, potentially varying from completely deterministic ($s=0$, conduits that are not embolized in one drought event will never be embolized in a subsequent similar event) to completely random ($s=1$, the mean probability of new embolism does not change regardless of the fraction of already embolized conduits).

The mass cost of xylem conductive tissue

The costs of xylem tissue are incurred by maintenance and construction, i.e. the structural investment in fibres and lignified tissues required (Sperry, 2003), which we assume to be proportional to mass. Xylem tissue consists of conduit walls and other cell types between the conduits. The thickness of conduit walls (T_c [μm]) is linked to tolerance to low water potential, ψ_{50}, and conduit diameter, D (Hacke et al., 2001). In angiosperms T_c may be constrained by the need to prevent wall implosion whereas the much thicker walls in gymnosperms may additionally be related to their role in providing overall stability (see Discussion). However, we found that T_c is best explained by a combination of ψ_{50}, and D (Table 2) so that

$$T_c = c_4\,\psi_{50}{}^f\,D^m. \tag{6}$$

If we assume that the density of conduit wall tissue (ρ) is constant, the mass (per unit length) of a conduit can be approximated by:

$$M = \rho\,\pi\,D\,T_c = c_5\,D^{m+1}\,\psi_{50}{}^f. \tag{7}$$

In the approximation we neglect the difference between outer and inner conduit diameter, which introduces only a minor error in the final results for optimal ψ_{50} at highly negative values of ψ_{min} (1.5% at ψ_{min} −10 MPa).

The optimal conduits

In addition to having a high conductivity per mass (K/M), optimal conduits should tolerate low ψ with minimal conductivity loss (embolism), that is P_t (Equation 5) should be as large as possible at the minimum operating water potential (ψ_{min}, the lowest ψ measured for a given site and species).
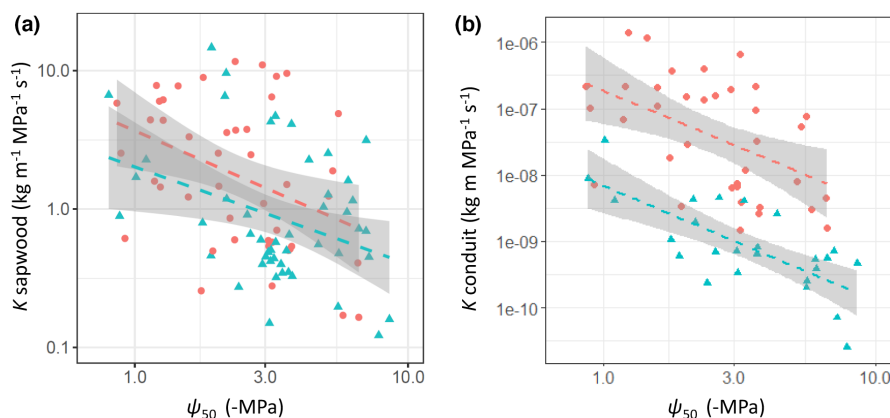

FIGURE 1 Trade-off between xylem tolerance to negative water potential (ψ_{50}) and maximal conductive capacity (K). Panels show measurements for whole sapwood (a) and for conduits only (b), which was calculated as sapwood conductivity/hydraulically weighted number of conduits per area (N, see above). Points show observations of angiosperms (red circles) and gymnosperms (blue-green triangles) and lines show standardized major axis regression (SMA) regressions with SE bands. $R^2=0.07$ and 0.12 for K sapwood (a) and 0.24 and 0.54 for K conduit (b), for angiosperms and gymnosperms, respectively. All p-values <0.003.

Since ψ_{min} reflects the integrated effect of water flux constraints due to environmental factors and plant stomatal behaviour, it exerts a strong selective force on the xylem (Bhaskar & Ackerly, 2006). Combining the two criteria for optimal xylem function—high conductive efficiency and high tolerance to low ψ—in the most parsimonious way, we obtain the optimality criterion, or fitness proxy F,

$$F = \frac{K}{M} \times P_t \text{ at } \psi = \psi_{min} \qquad (8)$$

We assume that F is optimized through the traits D and T_m, which together determine optimal ψ_{50}. Optimal D^* and T_m^* is obtained by maximization of F, i.e. dF/d$D=0$ and dF/d$T_m=0$ (Equations 9 and 10, derivation in Appendix S1).

$$D^* = \left(\frac{\psi_{min}}{c_2}\right)^{\frac{1}{d}} T_m^{\frac{-t}{d}} \left(\frac{x\,a\,d\,\ln(2)}{d\,f+m+1-k}\right)^{\frac{1}{d\,a}}. \qquad (9)$$

$$T_m^* = \left(\frac{\psi_{min}}{c_2}\right)^{\frac{1}{t}} D^{\frac{-d}{t}} \left(\frac{x\,a\,t\,\ln(2)}{t\,f-p}\right)^{\frac{1}{t\,a}}. \qquad (10)$$

Equations (9) and (10) both describe relationships between D^* and T_m^*. Based on the condition that both equations are consistent, that is there is coordinated optimality of D and T_m, we can calculate the undetermined parameter p (Equation 11) that determines the dependence of K on pit membrane thickness (Equation 1).

$$p = t\frac{k-m-1}{d}. \qquad (11)$$

By inserting the other parameter values (Table 1) in Equation (11), p can be calculated. $p=-0.94$ and -0.57 for angiosperms and gymnosperms, respectively, which means that K decreases with T_m (Equation 1).

The system of Equations (9) and (10) has no unique solution for D^* and T_m^*, which means that there is no single optimal combination of D^* and T_m^* for a given ψ_{min}, instead there is a relationship (curve) between the traits. Nevertheless, the equations do define a unique optimal ψ_{50} (Equation 12), which we calculate by inserting D^* (Equation 9) in Equation (3).

$$\psi_{50}^* = \psi_{min} \left(\frac{a\ln(2)\,x}{\frac{m+1-k}{d}+f}\right)^{\frac{1}{a}}. \qquad (12)$$

Because ψ_{50}^* does not depend on the role of T_m for either ψ_{50} (parameter t) or K (parameter p), Equation (12) for ψ_{50}^* would be valid even if there were no effect of T_m on conductivity, or if the equation for optimal T_m (Equation 10) were invalid.

In agreement with observations, Equation (12) implies a linear relationship between ψ_{min} and ψ_{50} with zero intercept, that is a constant ratio, or safety ratio $\psi_{50}/\psi_{min}=0.89$ for angiosperms and 1.69 for gymnosperms (Figure 2a,b).

Model evaluation

We evaluated the model in two steps. First, we used only observed ψ_{min} as a driver of predicted ψ_{50}, whereas all other parameters were constant, differing only between angiosperms and gymnosperms (Table 1). In a second analysis, we evaluated the model's ability to account for the additional non-linear effect of species- and site-specific values of the slope of the vulnerability curve (parameter a).

Whereas all other parameters were predetermined in the first analysis, the embolism accumulation parameter (x) was estimated by fitting the modelled ψ_{50}^* to observations, resulting in $x=0.96\pm0.047$ for angiosperms and $x=6.73\pm1.14$ for gymnosperms. The larger x indicates that gymnosperms are much more affected by embolism accumulation than angiosperms, which can be due to a lower capacity to refill embolized conduits (higher i), less variation in vulnerability among conduits with more stochasticity in the embolism process (higher s), or a larger number of expected drought events (n), or a combination of these factors. The difference in x was the main explanation for the larger safety ratio in gymnosperms than in angiosperms, whereas differences in other parameters are much smaller (Table 1). In addition to the interspecies variation, the model also explains the increase in negative ψ_{50} with ψ_{min} along the hydraulic path from roots to branches in two gymnosperm species (Figure 2c).

In the second analysis, the effect of variation in the parameter a was evaluated based on its effect on the safety ratio ψ_{50}/ψ_{min}, which is predicted to depend on a, i.e. $\frac{\psi_{50}^*}{\psi_{min}} = a^{\frac{1}{a}}\left(\frac{\ln(2)\,x}{\frac{m+1-k}{d}+f}\right)^{\frac{1}{a}}$ based on Equation (12). Importantly, the a values for each species were obtained from observations and x was the only fitted parameter (as in the first analysis). The ψ_{50}/ψ_{min} ratio increases exponentially for very small a values, peaks for low a values, and becomes essentially flat for high values of a (Figure 3). Although there is considerable variation, the observations follow the general shape of the theoretical predictions. To further illustrate the effect of variation in a, we re-evaluated the optimal ψ_{50} versus ψ_{min} relationships for different intervals of a, which shows the predicted variation in the slope with a (Figure 4). Including species specific values of a in the model fitting for angiosperms increased R^2 for modelled ψ_{50} to 0.59 compared to 0.48 in the model with constant a (Figure 2a). For gymnosperms, this did not improve R^2, which was expected due to the high a values falling on the flat part of the ψ_{50}/ψ_{min} curve (Figure 3b). The fitted values of x (1.02 for angiosperms and 4.07 for gymnosperms) differed only slightly from the first analysis.
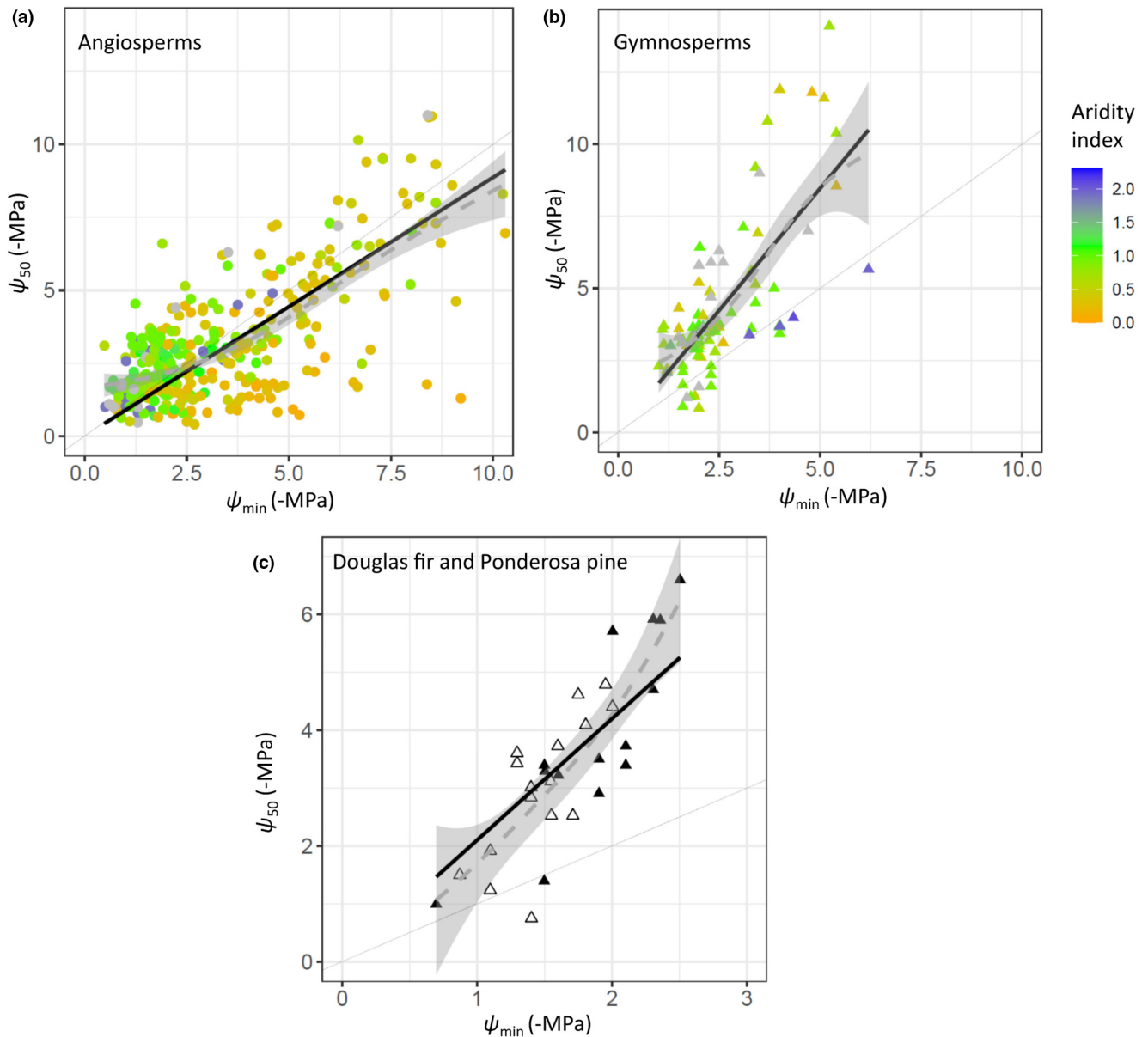
FIGURE 2 Observed and modelled xylem tolerance to negative water potential (ψ_{50}) versus minimum plant water potential (ψ_{min}). (a and b) Measurements in terminal branches for different species and sites, where colours indicate site aridity index (Annual precipitation/PET) from arid (orange) to wet (blue). Symbol shape indicates angiosperms (a, circles) and gymnosperms (b, triangles). (c) Measurements (means of 5–6 individuals) along the hydraulic path from roots, trunks and branches in Douglas fir (closed triangles) and Ponderosa pine (open triangles) (Domec et al., 2009). The dashed lines with shading show smoothed mean and SE intervals of the observed relationships. The straight thick lines are the model predictions (Equation 9). The thin black line is the 1:1 line. Modelled versus observed r^2 was 0.64 for Douglas fir and Ponderosa pine ($n=30$), 0.48 for angiosperms ($n=381$), and 0.50 for gymnosperms ($n=99$).

DISCUSSION

Optimal ψ_{50} determined by conductivity-safety trade-offs at the conduit level

It was previously not well explained why so many plants operate with such a narrow safety margin ($\psi_{50} - \psi_{min}$). Our model explains this phenomenon as the result of an optimal balancing of conductive capacity per biomass (K/M) and tolerance to low ψ. This trade-off differs from how hydraulic efficiency versus safety has been

analysed previously in two ways: (i) it includes the cost of conduits in terms of mass (M) as carbon investment, and (ii) it is applied at the level of individual conduits, or conduit tissue, rather than for the whole sapwood. Interestingly, the trade-off between conductive capacity (K) and ψ_{50} is much stronger at the conduit than at the sapwood level (Figure 1). Very weak trade-offs observed at the whole-sapwood level (Gleason et al., 2016) may be caused by the large variability among species in the number of conduits per sapwood area (Zanne et al., 2010). While safety (ψ_{50}) is primarily determined
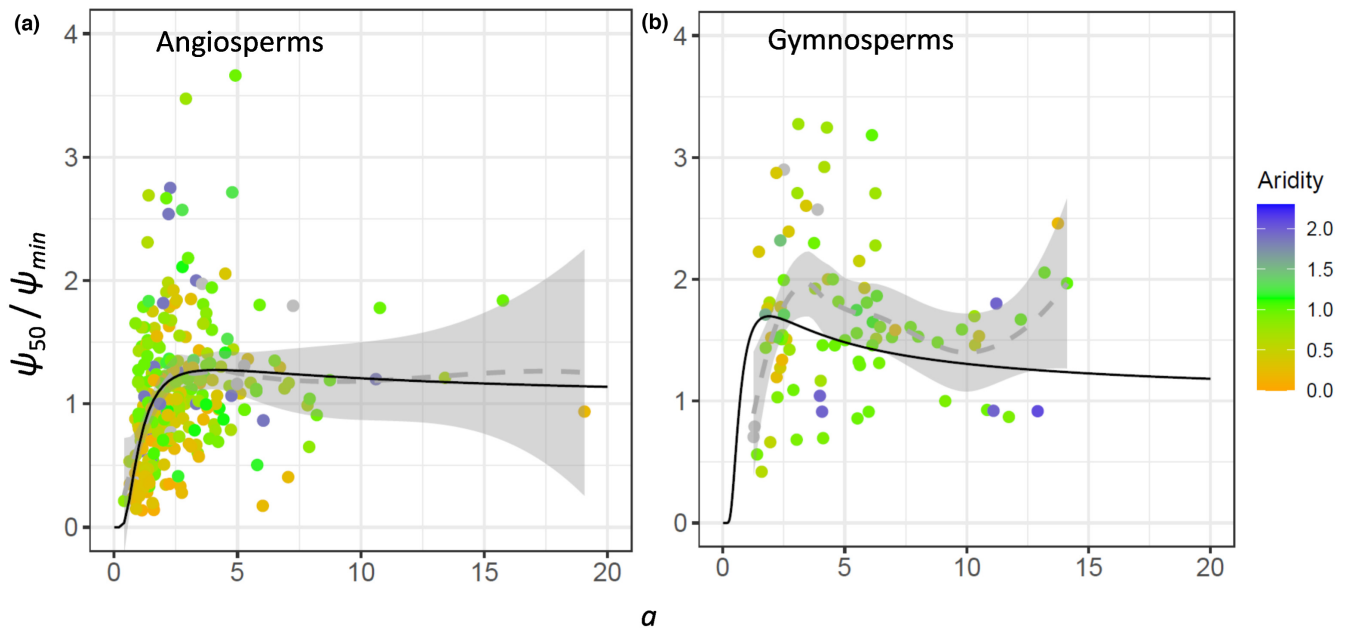
FIGURE 3　The effect of the slope of the vulnerability curve on the xylem hydraulic safety-ratio (ψ_{50}/ψ_{min}). The black line shows the theoretical prediction based on Equation (12). The dashed lines with shading show smoothed mean and SE intervals of the observed relationships. RMSE for modelled versus observed values = 0.58 for angiosperm and 0.67 for gymnosperms.
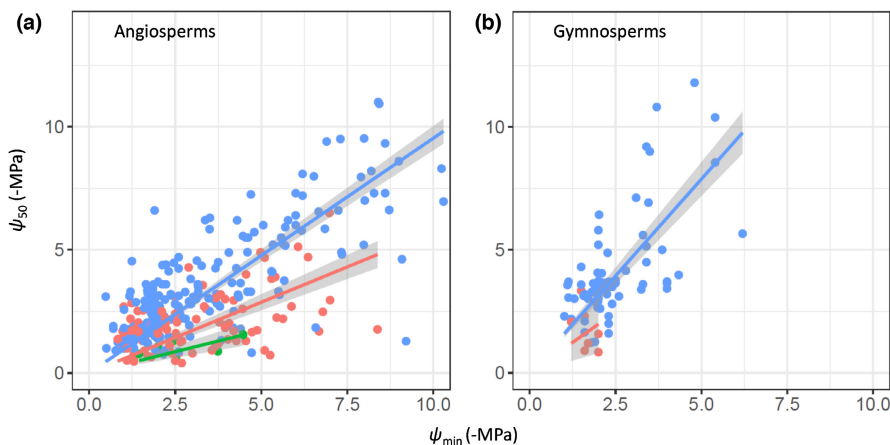

FIGURE 4　The effect of the slope of the vulnerability curve on embolism resistance (ψ_{50}) versus minimum plant water potential (ψ_{min}). The observations used in Figure 2a,b are split into intervals for the parameter a (the slope of the vulnerability function). For angiosperms $a < 0.8$ (green line), $0.8 < a < 1.6$ (red line), and $a > 1.6$ (blue line). For gymnosperms: $a < 1$ (no observations), $1 < a < 1.8$ (red line), and $a > 1.8$ (blue line). The intervals are based on the theoretical effect of a, implying a strongly increasing slope of ψ_{50} versus ψ_{min} for a less than ≈ 2 (Figure 3).

by traits at the pit and conduit level, whole sapwood conductivity increases proportionally with the number of conduits. However, even at the conduit level there is no perfect trade-off between K and ψ_{50} because there is not a 1:1 relationship between them. Instead, they are determined by two underlying traits: conduit diameter (D) and T_m (pit-membrane thickness in angiosperms, the ratio between torus and pit-membrane diameter in gymnosperms), which can vary under the constraints given by the optimality Equations (9) and (10). A given optimal ψ_{50} can thus be realized by different combinations of these two traits, corresponding to different K values and different conduit mass (M). Because these different trait combinations result in the same

hydraulic fitness, this mechanism may promote coexistence and diversity in hydraulic strategies. While T_m has mainly been studied with respect to ψ_{50} our model postulates that T_m scales negatively with K ($p < 0$ in Equation 1), implying that T_m is associated with a similar trade-off effect between conductivity and safety as D. There is at least some empirical support for the postulated negative effect of T_m on K (Lens et al., 2011; Trueba et al., 2019). However, in the face of our limited knowledge of the functional role of T_m it is important that our main result for optimal ψ_{50} does not hinge on optimality of T_m (Equation 10) or its relationship with K, because optimality of D only (Equation 9) is sufficient to derive optimal ψ_{50} (Equation 12).

Naturally, the number of traits included in our model is limited by the availability of data, allowing reliable quantification of effects and interrelationships for only a few traits. However, this limitation may not severely compromise the analysis if the modelled traits are representative and there is extensive coordination among traits, as has been observed (Sperry et al., 2006). Coordination and associated correlation imply that effects of non-modelled traits are implicitly accounted for via modelled traits, such as shown here for pit area and D (Table 2). Such coordination is expected from an eco-evolutionary point of view in order to avoid bottle necks in the conductive system as a whole, and may explain the link between D and ψ_{50} in the absence of a direct mechanism.

A constant ψ_{50}/ψ_{min} safety ratio across species and within individuals

The model provides a theoretical explanation and quantification of the previously observed general increase in the hydraulic safety margin with increasingly negative ψ_{min} (Choat et al., 2012; Meinzer et al., 2009), which results in an overall constant safety ratio (ψ_{50}/ψ_{min}) across species of the same type, i.e. angiosperms and gymnosperms (Figure 2). Some of the remaining variation in the safety ratio is explained by inter-species variation in the slope of the vulnerability curve (a), which is most relevant for angiosperms due to their wider range of a values extending to low values. For gymnosperms, variation in a has no significant effect on the safety ratio due to the higher range of a values (Figure 3). Whereas the correlation between ψ_{50} and ψ_{min} has been repeatedly confirmed, there are indications that some earlier studies included in our data set may have underestimated embolism resistance (ψ_{50}; Lens et al., 2022). A systematic bias in observed ψ_{50} would result in a slight overestimation of embolism accumulation (x) in our model, but it would not change any other results or conclusions.

Although relevant observations of variation in ψ_{min} and ψ_{50} within individuals are yet limited, our data suggest that the same optimality principle determines ψ_{50} both across different species and sites and along the xylem flow path in the stem within individuals (Figure 2c). The constant safety ratio may not extend to leaves, which often have a lower ratio corresponding to a segmentation of hydraulic vulnerability (Wason et al., 2018). Although not always recognized, segmentation is present even if leaves and stems have the same ψ_{50} because ψ will generally be more negative in the leaves (at the end of the hydraulic path) than in the stem.

Whereas the model captures well the overall trends in ψ_{50}, observed ψ_{50} is more negative than predicted by the model for less negative ψ_{min} (wet sites) (Figure 2a,b).

This bias could be related to an underestimation of negative ψ_{min} at wetter sites owing to lower sampling of rare dry days at such sites compared to more frequently occurring dry days at drier sites. Plants at wetter sites may be adapted to infrequent drought events that may be missed in the sampling of ψ_{min} (Martinez Vilalta et al., 2021).

The invariant ψ_{50}/ψ_{min} ratio predicted by our theory suggests that the presence of larger conduit diameters in taller plants (Olson et al., 2018) does not necessarily mean that they operate at a higher risk compared to shorter plants. Rather, our hypothesis suggests that taller plants with higher ψ_{50} should also experience a less negative ψ_{min} than shorter plants, which is in agreement with observations across a large number of species and environments (Liu et al., 2019). In a growing tree with increasing conduit diameters, optimal ψ_{50}/ψ_{min} ratio could be maintained by reducing negative ψ_{min} via increased whole xylem conductivity through additional conduits, more conservative stomatal regulation, or by means of increased water uptake with deeper roots, i.e. drought avoidance (Brum et al., 2017; Oliveira et al., 2021). Nevertheless, if these compensatory mechanisms are hampered by severe or prolonged drought, taller trees would still suffer more than shorter trees (Rowland et al., 2015).

Why do gymnosperms have a larger hydraulic safety ratio than angiosperms?

The model interprets the larger safety ratio ψ_{50}/ψ_{min} in gymnosperms compared to angiosperms (Figure 2) as an adaptation to stronger embolism accumulation (higher x in Equation 5). Our data and model do not allow us to separately estimate the underlying parameters contributing to this difference. However, observations suggest that two of our embolism accumulation parameters may be relevant: lack of refilling capacity (i) and variation in vulnerability among conduits (s). A negative relationship between safety ratio and refilling capacity has been observed in angiosperm trees (Ogasa et al., 2013; Trifilo et al., 2014) and may be related to the presence of axial rand ray parenchyma in xylem or phloem (Johnson et al., 2012; Kiorapostolou et al., 2019). However, although there are many records of embolism recovery in both angiosperms and gymnosperms (Klein et al., 2018), the significance of this process is under debate (Rehschuh et al., 2020).

The importance of vulnerability variation among conduits (parameter s) is supported by the recent finding that such variation leads to selective embolism of more vulnerable conduits, leaving the more resistant conduits functional, and therefore reducing the vulnerability of the remaining functional xylem to subsequent drought events (Avila et al., 2022). Only at very high levels of conductivity loss (>60%) this effect was overridden by

an opposite effect of embolism spreading through the xylem. The vulnerability-reducing selection effect was weaker in conifers (gymnosperms) than in angiosperms (Avila et al., 2022), which in our model leads to a higher s and a stronger embolism accumulation in gymnosperms (higher x in Equation 5), ultimately selecting for a higher safety ratio.

We also considered the possibility that the larger safety ratio in gymnosperms than angiosperms could be related to an additional role of conduit wall thickness to provide stem stability in gymnosperms. In this case, the steeper increase in wall thickness with diameter (m in Equation 6, Table 1) in gymnosperms would be related to stem stability rather than hydraulic function, and thus should not be included in the model for hydraulic fitness (Equation 8). However, accounting for this effect by setting m for gymnosperm tracheids equal to m for angiosperm conduits increases the safety ratio by only 2.6%, suggesting that unaccounted fitness-effects of conduit wall thickness are unlikely to explain the observed 88% difference in safety ratio between the plant types.

Conclusion

Our results show that the apparently risky hydraulic behaviour of plants in terms of narrow hydraulic safety margins can be explained as an eco-evolutionarily optimal design of xylem conduits. This result is rooted in a xylem conductive efficiency—safety trade-off at the scale of individual conduits related to conduit hydraulic diameter and pit-membrane traits. Optimal ψ_{50} is largely proportional to ψ_{min}, corresponding to a safety ratio $\psi_{50}/\psi_{min} \approx 0.9$ and 1.7 for angiosperms and gymnosperms, respectively. The model also explains part of the remaining variation in the safety ratio among species based on species-specific variation in the slope of the vulnerability curve. The optimal safety ratio holds across environments and species, and potentially also within stems of individual trees, and thus provides a powerful principle for simplifying and improving plant and vegetation models. The larger safety ratio in gymnosperms may be an adaptation to their larger tendency to suffer from accumulation of conductivity loss, due to lower refilling capacity or a smaller range of vulnerability among conduits. Our analysis highlights the need for further studies addressing the nature of conductivity loss accumulation. The optimality approach also demonstrates the importance of looking at xylem traits from both conductivity and safety perspectives in order to understand their costs and benefits.

AUTHOR CONTRIBUTIONS

Oskar Franklin conceived the original idea, analysed the data and wrote the draft manuscript. Jaideep Joshi and Peter Fransson contributed complementary mathematical analyses. Steven Jansen provided the main data set.

Florian Hofhansl and Jaideep Joshi provided complementary data. All authors contributed to conceptual development and the final manuscript.

PEER REVIEW
The peer review history for this article is available at https://www.webofscience.com/api/gateway/wos/peer-review/10.1111/ele.14270.

DATA AVAILABILITY STATEMENT
No new data were used. The combined data set and code used in this study are provided in a in a public repository: https://doi.org/10.5281/zenodo.7899749.

ORCID
Oskar Franklin https://orcid.org/0000-0002-0376-4140
Florian Hofhansl https://orcid.org/0000-0003-0073-0946

REFERENCES
Anderegg, W.R.L., Plavcová, L., Anderegg, L.D.L., Hacke, U.G., Berry, J.A. & Field, C.B. (2013) Drought's legacy: multiyear hydraulic deterioration underlies widespread aspen forest die-off and portends increased future risk. *Global Change Biology*, 19, 1188–1196.

Anderegg, W.R.L., Wolf, A., Arango-Velez, A., Choat, B., Chmura, D.J., Jansen, S. et al. (2018) Woody plants optimise stomatal behaviour relative to hydraulic risk. *Ecology Letters*, 21, 968–977.

Anfodillo, T., Carraro, V., Carrer, M., Fior, C. & Rossi, S. (2006) Convergent tapering of xylem conduits in different woody species. *The New Phytologist*, 169, 279–290.

Anfodillo, T. & Olson, M.E. (2021) Tree mortality: testing the link between drought, embolism vulnerability, and xylem conduit diameter remains a priority. *Frontiers in Forests and Global Change*, 109, 704670.

Avila, R.T., Guan, X., Kane, C.N., Cardoso, A.A., Batz, T.A., DaMatta, F.M. et al. (2022) Xylem embolism spread is largely prevented by interconduit pit membranes until the majority of conduits are gas-filled. *Plant, Cell and Environment*, 45, 1204–1215.

Bhaskar, R. & Ackerly, D.D. (2006) Ecological relevance of minimum seasonal water potentials. *Physiologia Plantarum*, 127, 353–359.

Bouche, P.S., Larter, M., Domec, J.-C., Burlett, R., Gasson, P., Jansen, S. et al. (2014) A broad survey of hydraulic and mechanical safety

in the xylem of conifers. *Journal of Experimental Botany*, 65, 4419–4431.

Brum, M., Teodoro, G., Abrahão, A. & Oliveira, R. (2017) Coordination of rooting depth and leaf hydraulic traits defines drought-related strategies in the Campos rupestres, a tropical montane biodiversity hotspot. *Plant and Soil*, 420, 1–14.

Choat, B., Cobb, A.R. & Jansen, S. (2008) Structure and function of bordered pits: new discoveries and impacts on whole-plant hydraulic function. *The New Phytologist*, 177, 608–626.

Choat, B., Jansen, S., Brodribb, T.J., Cochard, H., Delzon, S., Bhaskar, R. et al. (2012) Global convergence in the vulnerability of forests to drought. *Nature*, 491, 752–755.

Deans, R.M., Brodribb, T.J., Busch, F.A. & Farquhar, G.D. (2020) Optimization can provide the fundamental link between leaf photosynthesis, gas exchange and water relations. *Nature Plants*, 6, 1116–1125.

Domec, J.-C., Warren, J.M., Meinzer, F.C. & Lachenbruch, B. (2009) Safety factors for xylem failure by implosion and air-seeding within roots, trunks and branches of young and old conifer trees. *IAWA Journal*, 30, 101–120.

Duursma, R.A. & Choat, B. (2017) fitplc: an R package to fit hydraulic vulnerability curves. *Journal of Plant Hydraulics*, 4, e002.

Franklin, O., Harrison, S.P., Dewar, R., Farrior, C.E., Brännström, Å., Dieckmann, U. et al. (2020) Organizing principles for vegetation dynamics. *Nat. Plants*, 6, 444–453.

Gleason, S.M., Westoby, M., Jansen, S., Choat, B., Hacke, U.G., Pratt, R.B. et al. (2016) Weak tradeoff between xylem safety and xylem-specific hydraulic efficiency across the world's woody plant species. *The New Phytologist*, 209, 123–136.

Hacke, U.G., Sperry, J.S. & Pittermann, J. (2004) Analysis of circular bordered pit function II. Gymnosperm tracheids with torus-margo pit membranes. *American Journal of Botany*, 91, 386–400.

Hacke, U.G., Sperry, J.S., Pockman, W.T., Davis, S.D. & McCulloh, K.A. (2001) Trends in wood density and structure are linked to prevention of xylem implosion by negative pressure. *Oecologia*, 126, 457–461.

Hacke, U.G., Spicer, R., Schreiber, S.G. & Plavcová, L. (2017) An ecophysiological and developmental perspective on variation in vessel diameter. *Plant, Cell and Environment*, 40, 831–845.

Harrison, S.P., Cramer, W., Franklin, O., Prentice, I.C., Wang, H., Brännström, Å. et al. (2021) Eco-evolutionary optimality as a means to improve vegetation and land-surface models. *The New Phytologist*, 231, 2125–2141.

Hölttä, T., Mencuccini, M. & Nikinmaa, E. (2011) A carbon cost–gain model explains the observed patterns of xylem safety and efficiency. *Plant, Cell and Environment*, 34, 1819–1834.

Johnson, D.M., McCulloh, K.A., Woodruff, D.R. & Meinzer, F.C. (2012) Hydraulic safety margins and embolism reversal in stems and leaves: why are conifers and angiosperms so different? *Plant Science*, 195, 48–53.

Joshi, J., Stocker, B.D., Hofhansl, F., Zhou, S., Dieckmann, U. & Prentice, I.C. (2022) Towards a unified theory of plant photosynthesis and hydraulics. *Nature Plants*, 8, 1304–1316.

Kaack, L., Altaner, C.M., Carmesin, C., Diaz, A., Holler, M., Kranz, C. et al. (2019) Function and three-dimensional structure of intervessel pit membranes in angiosperms: a review. *IAWA Journal*, 40, 673–702.

Kaack, L., Weber, M., Isasa, E., Karimi, Z., Li, S., Pereira, L. et al. (2021) Pore constrictions in intervessel pit membranes provide a mechanistic explanation for xylem embolism resistance in angiosperms. *The New Phytologist*, 230, 1829–1843.

Kattge, J., Bönisch, G., Díaz, S., Lavorel, S., Prentice, I.C., Leadley, P. et al. (2020) TRY plant trait database–enhanced coverage and open access. *Global Change Biology*, 26, 119–188.

Kiorapostolou, N., Da Sois, L., Petruzzellis, F., Savi, T., Trifilò, P., Nardini, A. et al. (2019) Vulnerability to xylem embolism correlates to wood parenchyma fraction in angiosperms but not in gymnosperms. *Tree Physiology*, 39, 1675–1684.

Klein, T., Zeppel, M.J.B., Anderegg, W.R.L., Bloemen, J., De Kauwe, M.G., Hudson, P. et al. (2018) Xylem embolism refilling and resilience against drought-induced mortality in woody plants: processes and trade-offs. *Ecological Research*, 33, 839–855.

Koçillari, L., Olson, M.E., Suweis, S., Rocha, R.P., Lovison, A., Cardin, F. et al. (2021) The Widened Pipe Model of plant hydraulic evolution. *Proceedings of the National Academy of Sciences of the United States of America*, 118, e2100314118.

Lamy, J.-B., Delzon, S., Bouche, P.S., Alia, R., Vendramin, G.G., Cochard, H. et al. (2014) Limited genetic variability and phenotypic plasticity detected for cavitation resistance in a Mediterranean pine. *The New Phytologist*, 201, 874–886.

Lens, F., Gleason, S.M., Bortolami, G., Brodersen, C., Delzon, S. & Jansen, S. (2022) Functional xylem characteristics associated with drought-induced embolism in angiosperms. *The New Phytologist*, 236, 2019–2036.

Lens, F., Sperry, J.S., Christman, M.A., Choat, B., Rabaey, D. & Jansen, S. (2011) Testing hypotheses that link wood anatomy to cavitation resistance and hydraulic conductivity in the genus *Acer*. *The New Phytologist*, 190, 709–723.

Levionnois, S., Jansen, S., Wandji, R.T., Beauchêne, J., Ziegler, C., Coste, S. et al. (2021) Linking drought-induced xylem embolism resistance to wood anatomical traits in Neotropical trees. *The New Phytologist*, 229, 1453–1466.

Liu, H., Gleason, S.M., Hao, G., Hua, L., He, P., Goldstein, G. et al. (2019) Hydraulic traits are coordinated with maximum plant height at the global scale. *Science Advances*, 5, eaav1332.

Liu, H., Ye, Q., Gleason, S.M., He, P. & Yin, D. (2021) Weak tradeoff between xylem hydraulic efficiency and safety: climatic seasonality matters. *The New Phytologist*, 229, 1440–1452.

Lobo, A., Torres-Ruiz, J.M., Burlett, R., Lemaire, C., Parise, C., Francioni, C. et al. (2018) Assessing inter- and intraspecific variability of xylem vulnerability to embolism in oaks. *Forest Ecology and Management*, 424, 53–61.

Manzoni, S., Vico, G., Katul, G., Palmroth, S., Jackson, R.B. & Porporato, A. (2013) Hydraulic limits on maximum plant transpiration and the emergence of the safety–efficiency trade-off. *The New Phytologist*, 198, 169–178.

Martinez Vilalta, J., Santiago, L., Poyatos, R., Badiella, L., De Cáceres, M., Aranda, I. et al. (2021) Towards a statistically robust determination of minimum water potential and hydraulic risk in plants. *The New Phytologist*, 232, 404–417.

McCulloh, K.A., Sperry, J.S. & Adler, F.R. (2003) Water transport in plants obeys Murray's law. *Nature*, 421, 939–942.

Meinzer, F.C., Johnson, D.M., Lachenbruch, B., McCulloh, K.A. & Woodruff, D.R. (2009) Xylem hydraulic safety margins in woody plants: coordination of stomatal control of xylem tension with hydraulic capacitance. *Functional Ecology*, 23, 922–930.

Ogasa, M., Miki, N.H., Murakami, Y. & Yoshikawa, K. (2013) Recovery performance in xylem hydraulic conductivity is correlated with cavitation resistance for temperate deciduous tree species. *Tree Physiology*, 33, 335–344.

Oliveira, R.S., Eller, C.B., Barros, F.d.V., Hirota, M., Brum, M. & Bittencourt, P. (2021) Linking plant hydraulics and the fast–slow continuum to understand resilience to drought in tropical ecosystems. *The New Phytologist*, 230, 904–923.

Olson, M.E., Soriano, D., Rosell, J.A., Anfodillo, T., Donoghue, M.J., Edwards, E.J. et al. (2018) Plant height and hydraulic vulnerability to drought and cold. *Proceedings of the National Academy of Sciences of the United States of America*, 115, 7551–7556.

Pellizzari, E., Camarero, J.J., Gazol, A., Sangüesa-Barreda, G. & Carrer, M. (2016) Wood anatomy and carbon-isotope discrimination support long-term hydraulic deterioration as a major cause of drought-induced dieback. *Global Change Biology*, 22, 2125–2137.

Pritzkow, C., Williamson, V., Szota, C., Trouvé, R. & Arndt, S.K. (2020) Phenotypic plasticity and genetic adaptation of functional traits influences intra-specific variation in hydraulic efficiency and safety. *Tree Physiology*, 40, 215–229.

Rehschuh, R., Cecilia, A., Zuber, M., Faragó, T., Baumbach, T., Hartmann, H. et al. (2020) Drought-induced xylem embolism limits the recovery of leaf gas exchange in scots pine. *Plant Physiology*, 184, 852–864.

Rowland, L., da Costa, A.C.L., Galbraith, D.R., Oliveira, R.S., Binks, O.J., Oliveira, A.A.R. et al. (2015) Death from drought in tropical forests is triggered by hydraulics not carbon starvation. *Nature*, 528, 119–122.

Sanchez-Martinez, P., Martínez-Vilalta, J., Dexter, K.G., Segovia, R.A. & Mencuccini, M. (2020) Adaptation and coordinated evolution of plant hydraulic traits. *Ecology Letters*, 23, 1599–1610.

Savage, V.M., Bentley, L.P., Enquist, B.J., Sperry, J.S., Smith, D.D., Reich, P.B. et al. (2010) Hydraulic trade-offs and space filling enable better predictions of vascular structure and function in plants. *Proceedings of the National Academy of Sciences of the United States of America*, 107, 22722–22727.

Scholz, A., Rabaey, D., Stein, A., Cochard, H., Smets, E. & Jansen, S. (2013) The evolution and function of vessel and pit characters with respect to cavitation resistance across 10 Prunus species. *Tree Physiology*, 33, 684–694.

Sperry, J.S. (2003) Evolution of water transport and xylem structure. *International Journal of Plant Sciences*, 164, 115–127.

Sperry, J.S., Hacke, U.G. & Pittermann, J. (2006) Size and function in conifer tracheids and angiosperm vessels. *American Journal of Botany*, 93, 1490–1500.

Trifilo, P., Barbera, P., Raimondo, F., Nardini, A. & Lo Gullo, M.A. (2014) Coping with drought-induced xylem cavitation: coordination of embolism repair and ionic effects in three Mediterranean evergreens. *Tree Physiology*, 34, 109–122.

Trueba, S., Delzon, S., Isnard, S. & Lens, F. (2019) Similar hydraulic efficiency and safety across vesselless angiosperms and vessel-bearing species with scalariform perforation plates. *Journal of Experimental Botany*, 70, 3227–3240.

Venturas, M.D., Sperry, J.S. & Hacke, U.G. (2017) Plant xylem hydraulics: what we understand, current research, and future challenges. *Journal of Integrative Plant Biology*, 59, 356–389.

Wang, H., Prentice, I.C., Keenan, T.F., Davis, T.W., Wright, I.J., Cornwell, W.K. et al. (2017) Towards a universal model for carbon dioxide uptake by plants. *Nature Plants*, 3, 734–741.

Wang, Y., Sperry, J.S., Anderegg, W.R.L., Venturas, M.D. & Trugman, A.T. (2020) A theoretical and empirical assessment of stomatal optimization modeling. *The New Phytologist*, 227, 311–325.

Wason, J.W., Anstreicher, K.S., Stephansky, N., Huggett, B.A. & Brodersen, C.R. (2018) Hydraulic safety margins and air-seeding thresholds in roots, trunks, branches and petioles of four northern hardwood trees. *The New Phytologist*, 219, 77–88.

West, G.B., Brown, J.H. & Enquist, B.J. (1999) A general model for the structure and allometry of plant vascular systems. *Nature*, 400, 664–667.

Wheeler, J.K., Sperry, J.S., Hacke, U.G. & Hoang, N. (2005) Intervessel pitting and cavitation in woody Rosaceae and other vesselled plants: a basis for a safety versus efficiency trade-off in xylem transport. *Plant, Cell and Environment*, 28, 800–812.

Wolf, A., Anderegg, W.R.L. & Pacala, S.W. (2016) Optimal stomatal behavior with competition for water and risk of hydraulic impairment. *Proceedings of the National Academy of Sciences of the United States of America*, 113, E7222–E7230.

Zanne, A.E., Westoby, M., Falster, D.S., Ackerly, D.D., Loarie, S.R., Arnold, S.E.J. et al. (2010) Angiosperm wood structure: global patterns in vessel anatomy and their relation to wood density and potential conductivity. *American Journal of Botany*, 97, 207–215.

Zhang, Q.-W., Zhu, S.-D., Jansen, S. & Cao, K.-F. (2021) Topography strongly affects drought stress and xylem embolism resistance in woody plants from a karst forest in Southwest China. *Functional Ecology*, 35, 566–577.

SUPPORTING INFORMATION

Additional supporting information can be found online in the Supporting Information section at the end of this article.